

Use of Ar⁺ Plasma Etching To Localize Structural Proteins in the Capsid of Herpes Simplex Virus Type 1

WILLIAM W. NEWCOMB AND JAY C. BROWN*

Department of Microbiology and Cancer Center, University of Virginia Health Sciences Center, Charlottesville, Virginia 22908

Received 16 May 1989/Accepted 31 July 1989

Partially cored herpes simplex virus type 1 (HSV-1) capsids (B capsids) were eroded in a low-energy (0.5-keV) Ar⁺ ion plasma under conditions in which the outermost structural proteins were expected to be degraded before more internal ones. After various periods of etching, the proteins remaining intact were separated by sodium dodecyl sulfate-polyacrylamide gel electrophoresis and determined quantitatively by densitometric scanning of the stained gels. The results showed that the major capsid polypeptide (VP5) and two other capsid proteins, VP19 and VP23, were degraded rapidly beginning as soon as capsids were exposed to the ion plasma. In contrast, significant lags were observed for erosion of VP21, VP22a, and VP24, suggesting that these proteins were available to accelerated ions only after other, more external structures had been damaged or eroded away. The results suggest that VP5, VP19, and VP23 are exposed on the surface of the capsid, while VP21, VP22a, and VP24 are found inside the capsid cavity. The experiments are consistent with the view that VP5 constitutes the major structural component of the hexavalent capsomers. It is proposed that VP19 and VP23 may form other surface structures such as the pentavalent capsomers, the capsid floor, or the intercapsomeric fibers.

Capsid architecture is among the most characteristic features of the herpesvirus family. In all herpesvirus species examined the capsid is icosahedral with a wall approximately 14 nm thick and a "diameter" of 105 to 116 nm (4, 8). Capsids consist of exactly 162 capsomers (triangulation number, 16) arranged in such a way that 150 capsomers, the hexavalent capsomers, form the edges and faces of the icosahedron and have six nearest neighbors (25). The remaining 12 capsomers, the pentavalent capsomers, are located at the capsid vertices and have five nearest neighbors. Capsomers are connected by Y-shaped fibers linking the capsomers in groups of three and centered at points equidistant from three capsomers (21). In the intact virus the capsid encloses the viral DNA and is surrounded by the tegument and by a glycoprotein-containing membrane. Recent cryo-electron microscopic studies by Schrag et al. (21) have suggested that there is an icosahedral shell (triangulation number, 4) between the capsid and the DNA mass.

Capsids can be isolated in high yield from the nuclei of herpesvirus-infected cells. Like several other herpesvirus species, herpes simplex virus type 1 (HSV-1)-infected cells yield capsids of three distinct types, called A, B, and C (7). These have the same basic architecture but differ in sedimentation rate, amount of material in the capsid cavity, and ability to mature into infectious virions. For example, whereas A capsids do not contain DNA, B (partially cored) capsids contain a significant amount of internal material and, at least in equine herpesvirus type 1 (EHV-1), can mature into intact virions (17). C (filled) capsids contain the entire DNA genome and are also maturable.

Biochemical analyses have demonstrated that HSV-1 B capsids consist of seven distinct protein species. One of these, called the major capsid protein or VP5 (M_r , 149,075; 12), constitutes approximately 60% of the total capsid mass

and is thought to be the basic structural component of the hexavalent capsomers (24). Three other proteins, VP19, VP22a, and VP23, together account for approximately 35% of the capsid mass, but their locations in the native structure are less certain. One or more could constitute the pentavalent capsomers, the protein fibers connecting adjacent capsomers, the "floor" material in which capsomers appear to be embedded, or the internal contents of the capsid cavity.

The studies described here were undertaken to clarify the location of B-capsid structural proteins by application of the Ar⁺ plasma etching technique recently developed in our laboratory (13). Intact capsids were exposed to low energy Ar⁺ plasmas (glow discharges) under conditions in which the outermost polypeptides were expected to be degraded before internal ones. Irradiated capsids were then analyzed by sodium dodecyl sulfate (SDS)-polyacrylamide gel electrophoresis to measure the amount of each polypeptide damaged by ion bombardment. Success of the method depends on the fact that Ar⁺ ions in the energy range employed (approximately 0.5 keV) are able to break chemical bonds and erode material from the particle surface, although their range of penetration is small (2.2 to 4.4 nm) compared with the capsid diameter (15). Analysis of experimentally determined protein decay curves has allowed us to classify six capsid polypeptides as exposed on the surface or as protected inside the capsid wall.

MATERIALS AND METHODS

Virus growth and capsid purification. All experiments were carried out with HSV-1 strain 17MP (obtained in 1986 from Glenn Gentry, University of Mississippi) which was grown at 37°C on monolayer cultures of BHK-21 cells. The cells were propagated in Dulbecco modified minimal essential medium (DMEM) containing 8% newborn calf serum and antibiotics. Capsids were prepared beginning with log-phase (75% confluent) cell cultures which were grown in 850-cm²

* Corresponding author.

roller bottles and infected with 1.5 ml of virus stock (at a multiplicity of infection of 1 to 4 PFU per cell). The virus was first allowed to attach to cells for 30 min; infection was then continued for 15 h at 37°C in 50 ml of DMEM containing 2% calf serum and 10% tryptose phosphate broth. B capsids were isolated from the nuclei of infected cells essentially by the method of Perdue et al. (16). This procedure involved disruption of cell nuclei by sonication and separation of A, B, and C capsids by centrifugation on a Renografin-76 gradient. After centrifugation, the band of B capsids was removed from the gradient with a Pasteur pipette, diluted in TE buffer (10 mM Tris hydrochloride [pH 7.4], 1 mM EDTA), and pelleted by centrifugation for 1 h at 24,000 rpm in an SW28 rotor. Typical preparations beginning with five roller bottles of infected cells yielded 1 to 2 mg of purified B capsids which were found, by electron microscopic analysis of negatively stained preparations (23), to contain less than 10% A capsids and 5% or less C capsids.

Ar⁺ etching. B-capsid samples were prepared for Ar⁺ plasma etching by being freeze-dried on plastic cover slips (2.2 by 2.2 cm) as previously described (13). Each cover slip contained 5 to 10 µg of purified B capsids, or enough to cover 10 to 20% of the cover slip area. Cover slips containing freeze-dried capsids were etched capsid side up on the cathode of a modified Polaron E5100 sputter coater (13) operated at 5 mA (approximately 500 V) in 100% Ar at 100 mtorr (13.3 Pa). Under these conditions the penetration depth of Ar⁺ ions is expected to be 2.2 to 4.4 nm (15). Etching times were determined empirically. After etching was complete, capsid proteins were removed from cover slips by incubation at 60°C in SDS-polyacrylamide gel sample buffer (2% SDS, 1.5% dithiothreitol, 20% glycerol, 25 mM Tris hydrochloride [pH 8.8]) as previously described (13).

Gel electrophoresis, protein quantitation, and measurement of decay rates. SDS-polyacrylamide gel electrophoresis was carried out with proteins removed from four to eight cover slips. These samples (40 to 50 µl) were boiled for 2 min and analyzed by electrophoresis on 10% polyacrylamide slab gels (10 cm by 13 cm by 1.5 mm), using the Laemmli (10) buffer system. Previously described procedures (13) were employed for staining gels with 0.4% Coomassie brilliant blue, destaining, and measuring the amount of protein in stained bands by densitometric scanning with the LKB UltraScan laser densitometer. For each protein analyzed, the amount present in etched specimens was expressed as a fraction of the amount found in control, unetched capsids, which was taken to be 1.00. Gel analyses of proteins from freeze-dried and undried capsids were found to be closely similar. For example, in comparable analyses of the two, no protein was found to differ in amount by more than 10%. Thus, there was no evidence for systematic resistance of particular proteins to solubilization after being freeze-dried.

Protein decay rates were measured from the initial, logarithmic portions of the overall decay curves. The observed first-order decay rates were corrected for the effect of protein target size, assuming that all proteins were spherical and that target size was proportional to surface area. Protein molecular weights used were those given by Gibson and Roizman (7), except for the molecular weight of VP5, which was taken from McGeoch et al. (12).

Electron microscopy. Electron microscopy was performed with capsid samples that were adsorbed to carbon-Formvar-coated copper electron microscope grids (400 mesh), critical point dried without fixation in a Tousimis samdri 780 critical point dryer, and etched (if necessary) as described above on a glass support. Dried capsids were then rotary shadowed

with Pt-C at a 70° angle in a Balzers BAE 080 vacuum evaporator and photographed at 26,000× in a JEOL 100cx transmission electron microscope.

RESULTS

The B capsids employed in this study were characterized by electron microscopy of shadowed preparations and by SDS-polyacrylamide gel electrophoresis. Electron microscopic analysis (Fig. 1a) revealed that the capsids were quite homogeneous in morphology and relatively free from contaminating noncapsid material. In most cases their icosahedral shape could be discerned and individual capsomers could be seen to protrude above a floor or base layer. After etching for 10 s (the maximum time employed in this study), there was clear evidence that individual capsomers had been eroded or smoothed (Fig. 1b, arrows). The overall icosahedral capsid morphology was still clearly evident, however, and reduction in the capsid "diameter" was less than 10%. SDS-polyacrylamide gel analyses of unetched capsids demonstrated the presence of the six expected polypeptides (Table 1; Fig. 2, lane 1), which together accounted for 90% or more of the total protein present. Their relative abundance (Table 1) was in the range of values previously reported for B capsids (7). The 12-kilodalton polypeptide (VP26) reported by Cohen et al. (3) either was not present in our preparations or migrated at the bromophenol blue dye front.

Figure 2 shows the results of SDS-polyacrylamide gel analyses performed with capsids that had been etched for various times in a 0.5-keV Ar⁺ plasma. Yields of the six major proteins are shown quantitatively as a function of etching time in Fig. 3 and in the form of first-order rate (decay) constants in Table 2. From an examination of the stained gels (Fig. 2) one could see that VP5 and VP19 were lost rapidly as a function of etching time, while erosion of VP22a and VP24 was much slower. In all etched specimens (Fig. 2, lanes 2 through 5) there was a marked accumulation of stained material between the major protein bands. Much of this material was present as a smear, but occasionally distinct bands were evident. Two of these bands are indicated by asterisks in Fig. 2, lane 2. Such bands most probably correspond to polypeptides produced by preferential cleavage of larger proteins at defined sites. (Thus, the bands indicated by asterisks in Fig. 2, lane 2, are expected to be derived from VP5, since this is the only larger protein.) Erosion of the major protein species was also accompanied by an increase in the amount of stainable material, most probably small degradation products, migrating at the bromophenol blue dye front.

Quantitative analysis of the stained gels revealed that degradation of capsid proteins followed one of two quite different kinetic courses (Fig. 3). Loss of VP5, VP19, and VP23 began as soon as capsids were exposed to accelerated ions and proceeded more or less logarithmically until less than 20% of the original protein remained (approximately 6 s of etching). In contrast, biphasic kinetics were observed for degradation of VP21, VP22a, and VP24. Their loss was slow during the initial 1 to 3 s of etching and more rapid thereafter. First-order rate constants (Table 2) calculated from the initial slopes (in two experiments) showed that proteins lost with monophasic kinetics (VP5, VP19, and VP23) had rates of 0.31 to 0.80 s⁻¹, while those for VP21, VP22a, and VP24 were 0.02 to 0.14 s⁻¹. After correction for protein target size, the corresponding values were 0.69 to 1.31 s⁻¹ and 0.07 to 0.37 s⁻¹, respectively. In both experiments, corrected

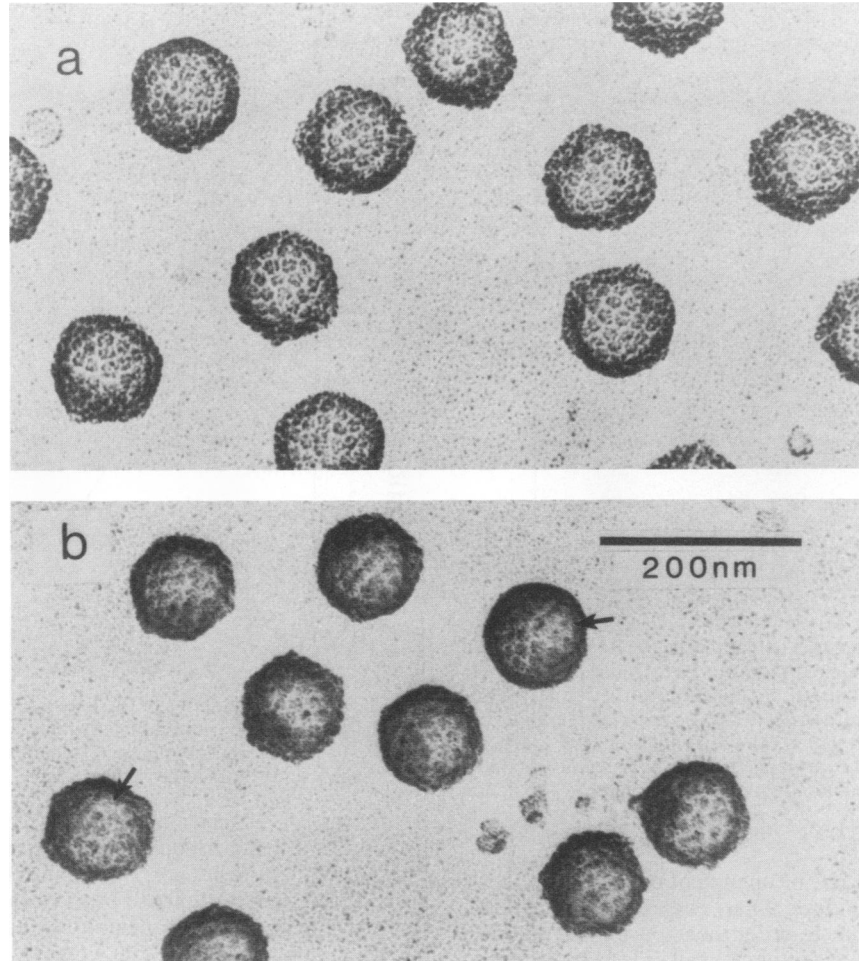


FIG. 1. Electron micrographs of HSV-1 B capsids before (a) and after (b) Ar^+ etching. B capsids were purified, critical point dried, etched (for 10 s), and shadowed with Pt-C as described in Materials and Methods. Arrows in panel b indicate regions where capsomers can be seen to be eroded by the etching process.

rate constants were higher for VP19 and VP23 than for VP5. The largest inconsistency between the two experiments was observed in the case of VP24, which had corrected rate constants of 0.07 s^{-1} and 0.37 s^{-1} . In all other cases, the corrected rate constants differed by 50% or less in two experiments.

TABLE 1. Protein composition of HSV-1 B capsids^a

Protein	$M_r, 10^3$	% of total protein ^b		
		Expt 1	Expt 2	Avg
5	149	51.7	72.1	61.9
19	53	10.6	8.2	9.4
21	44	2.2	1.9	2.1
22a	39	23.6	7.2	15.4
23	33	10.8	9.6	10.2
24	25	1.1	1.0	1.0

^a The procedures employed for B-capsid preparation, protein solubilization, gel electrophoresis, and protein quantitation are described in Materials and Methods.

^b Capsids were considered to consist only of the six indicated proteins. Material migrating at the dye front and minor polypeptides (which accounted for less than 1% of the stained protein) were not included in the analysis.

DISCUSSION

The most significant feature of the results reported here is the time at which erosion of individual capsid proteins began. VP5, VP19, and VP23 were degraded beginning as soon as capsids were exposed to accelerated ions, suggesting that all or part of these polypeptides was either exposed directly on the capsid surface or lay close enough to the surface to be initially within the range (2.2 to 4.4 nm) of accelerated ions. In contrast, there was a distinct lag or delay (biphasic kinetics) in the loss of VP21, VP22a, and VP24. These proteins must, therefore, have been buried deeply enough that they were initially beyond the range of Ar^+ ions. The delay observed for their loss most probably represents the time required for more external structures to be damaged or eroded away (13).

It is of lesser significance that the corrected decay constants for VP19 and VP23 were higher than that for VP5. In principle, this indicates that the ratio of exposed surface area to protein mass is greater for VP19 and VP23 than for VP5. In fact, however, the small rate differences observed may be due to secondary factors such as deviations of proteins from the assumed spherical geometry, partial shielding of one

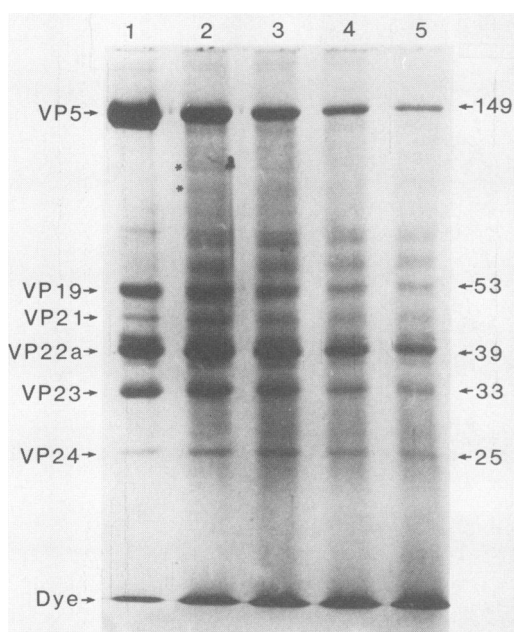


FIG. 2. SDS-polyacrylamide gel analysis of HSV-1 B capsid proteins derived from unetched capsids (lane 1) and from capsids etched for 1 s (lane 2), 3 s (lane 3), 6 s (lane 4), and 10 s (lane 5). Gels were run and stained with Coomassie blue as described in Materials and Methods. Molecular weights (MW; in thousands) of the major polypeptide species are shown to the right. The asterisks in lane 2 indicate polypeptides thought to be derived from VP5 by the action of accelerated ions.

surface protein by another, or alignment of proteins relative to the direction of incident ions. The results, therefore, probably do not allow one to order the exposed polypeptides according to their relative degree of availability on the capsid surface.

In formulating the above interpretation it was assumed that erosion of capsids in the ion plasma was more or less geometrically uniform. Studies with model substrates such as yeast cells and polystyrene spheres have suggested that the assumption is justified. These materials were found to be eroded in an isotropic or omnidirectional manner when they were irradiated on nonconducting supports at voltages of less than 5 to 10 keV (W. Newcomb and J. Brown, unpublished observations). Both conditions applied in the present study. Moreover, direct electron microscopic analysis of etched capsids (Fig. 1b) supported the view that erosion had taken place from all directions.

Our conclusion that VP5 lies at or very near the capsid surface is consistent with the idea that it forms the major structural component of the hexavalent (and also possibly pentavalent) capsomers (24). It is most likely, therefore, that the other exposed polypeptides, VP19 and VP23, constitute the remaining structural features of the capsid surface. These could include the pentavalent capsomers (if they are not composed of VP5), the trigonal, fiberlike material found to connect adjacent capsomers (21), and the floor or base material in which capsomers appear to be embedded. The properties of VP19 make it an attractive candidate for the floor material. Its ability to bind DNA (1) and its disulfide bond(s) to the major capsid protein (26) would both be accommodated if it were to anchor capsomers on the outer side of the capsid wall while making contact with DNA inside. Although less is known about the properties of VP23,

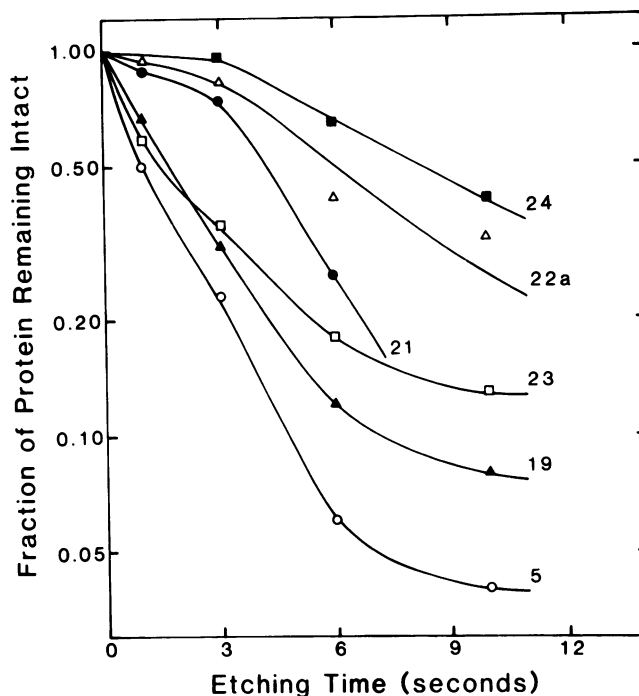


FIG. 3. Decay kinetics of the major proteins during Ar^+ etching of HSV-1 B capsids. Individual proteins were determined quantitatively by densitometric scanning (as described in Materials and Methods) of the stained gel shown in Fig. 2.

it could form the trigonal, intercapsomeric material as suggested by Schrag et al. (21). The number of VP23 molecules per capsid expected on the basis of this model (960) is close to the range of experimental values (9, 14) reported for EHV-1 (approximately 700 copies) and HSV-1 (1,400 to 1,700 copies) capsids.

From the total amount of VP19 and VP23 found to be present in B capsids, one can argue that neither could constitute only the pentavalent capsomers. For example, if the total mass of HSV-1 B capsids is comparable to that of EHV-1 intermediate capsids (which are closely similar in other respects), then one can calculate that B capsids must contain approximately 21 megadaltons of VP19 and 23

TABLE 2. First-order rate constants for degradation of HSV-1 capsid proteins during Ar^+ plasma etching of intact capsids^a

Protein	Rate constant (s^{-1})		Rate constant (s^{-1}) corrected for protein target size ^b	
	Expt 1	Expt 2	Expt 1	Expt 2
VP5	0.69	0.80	0.69	0.80
VP19	0.40	0.64	0.82	1.31
VP21	0.12	0.06	0.28	0.14
VP22a	0.08	0.14	0.20	0.35
VP23	0.36	0.31	1.00	0.86
VP24	0.02	0.11	0.07	0.37

^a All Ar^+ plasma etching was carried out at 5 mA as described in Materials and Methods. Rate constants were calculated from the initial portions of logarithmic decay curves such as those shown in Fig. 3. Data in Fig. 3 correspond to experiment 1.

^b Observed rate constants were corrected for the effects of protein target size by assuming that all proteins were spherical and that target size was proportional to protein surface area (i.e., proportional to molecular weight \times 2/3). Corrections were made relative to the value for VP5 (M_r , 149,075).

megadaltons of VP23 (14). This contrasts with a total mass of 9.6 megadaltons measured by Schrag et al. (21) for the 12 pentavalent capsomers. Thus, if either VP19 or VP23 forms the pentavalent capsomers, then it must also be present elsewhere in the capsid structure. Gibson's studies with cytomegalovirus provide further evidence that VP19 is unlikely to constitute the pentamers. Cytomegalovirus B capsids were found to have morphologically normal pentamers despite the fact that they lack a polypeptide analogous to HSV-1 VP19 (5, 6).

The internal localization of VP22a as indicated by the evidence presented here is in conflict with the surface-labeling study of Braun et al. (2). These investigators observed that VP22a was iodinated when B capsids were reacted in vitro with particle-bound lactoperoxidase and concluded that VP22a was exposed on the capsid surface. The reasons for the discrepancy with the present study are not yet clear. It is possible that the VP22a molecules iodinated in the earlier study (2) were free in solution or were present in broken or damaged capsids. The view that VP22a is located inside B capsids, however, is supported by electron microscopic analyses of rotary-shadowed HSV-1 A and B capsids. No detectable differences were observed in the surface architecture of these structures (both resembled the images shown in Fig. 1a) despite the fact that A capsids lack VP22a (W. Newcomb and J. Brown, unpublished observations). Similar results were obtained with shadowed preparations of EHV-1 light and intermediate capsids, which resemble HSV-1 A and B capsids, respectively (14). Finally, no evidence for surface VP22a was obtained when cryo-electron microscopic images of EHV-1 light and intermediate capsids were employed to compute three-dimensional reconstructions of the two capsid types at high resolution (T. S. Baker, W. W. Newcomb, F. P. Booy, J. C. Brown, and A. C. Steven, in *Proceedings of the 47th Meeting of the Electron Microscopy Society of America*, abstr., p. 822-823, 1989). These latter results (together with the present ion-etching study) are most compatible with the view that VP22a is found inside the capsid cavity. There it could constitute the variously shaped structures observed near the capsid center in thin sections of purified B capsids and of B capsids in infected-cell nuclei (7, 20). The internal localization of VP22a as suggested here is in accord with its proposed role in DNA packaging (18, 19, 22) or as a scaffolding or assembly protein involved in capsid morphogenesis (11).

The two remaining internal polypeptides, VP21 and VP24, are quite minor components of the B capsid. Together they account for less than 5% of the total capsid mass (Table 1; 7), and little is known about the function of VP24. The proposed location of VP21 inside the capsid wall is compatible with the idea that it may be a partially processed form of VP22a (1) or that it may form the proteinaceous core around which the DNA appears to be wrapped in the mature virion (7).

ACKNOWLEDGMENTS

We thank Wade Gibson, John Boring, Alasdair Steven, and Jace Houglund for productive discussions about this project.

This work was supported by Public Health Service grant GM34036 from the National Institutes of Health.

LITERATURE CITED

- Braun, D. K., W. Batterson, and B. Roizman. 1984. Identification and genetic mapping of a herpes simplex virus capsid protein that binds DNA. *J. Virol.* **50**:645-648.
- Braun, D. K., B. Roizman, and L. Pereira. 1984. Characterization of post-translational products of herpes simplex virus gene 35 proteins binding to the surfaces of full capsids but not empty capsids. *J. Virol.* **49**:142-153.
- Cohen, G., M. Ponce de Leon, H. Diggelmann, W. Lawrence, S. K. Vernon, and R. Eisenberg. 1980. Structural analysis of the capsid polypeptides of herpes simplex viruses types 1 and 2. *J. Virol.* **34**:521-531.
- Dargan, D. J. 1986. The structure and assembly of herpesviruses, p. 359-437. In J. Harris and R. Horne (ed.), *Electron microscopy of proteins*, vol. 5. Academic Press, Inc. (London), Ltd., London.
- Gibson, W. 1981. Structural and nonstructural proteins of strain Colburn cytomegalovirus. *Virology* **111**:516-537.
- Gibson, W. 1983. Protein counterparts of human and simian cytomegaloviruses. *Virology* **128**:391-406.
- Gibson, W., and B. Roizman. 1972. Proteins specified by herpes simplex virus. VIII. Characterization and composition of multiple capsid forms of subtypes 1 and 2. *J. Virol.* **10**:1044-1052.
- Hay, J., C. R. Roberts, W. T. Ruyechan, and A. C. Steven. 1987. Herpesviridae, p. 391-405. In M. Nermut and A. Steven (ed.), *Animal virus structure*. Elsevier, Amsterdam.
- Heine, J. W., R. W. Honess, E. Cassai, and B. Roizman. 1974. Proteins specified by herpes simplex virus. XII. The virion polypeptides of type 1 strains. *J. Virol.* **14**:640-651.
- Laemmli, U. K. 1970. Cleavage of structural proteins during the assembly of the head of bacteriophage T4. *Nature (London)* **227**:680-685.
- Lee, J. Y., A. Irmiere, and W. Gibson. 1988. Primate cytomegalovirus assembly: evidence that DNA packaging occurs subsequent to B capsid assembly. *Virology* **167**:87-96.
- McGeoch, D. J., M. A. Dalrymple, A. J. Davidson, A. Dolan, M. C. Frame, D. McNab, L. J. Perry, J. A. Scott, and P. Taylor. 1988. The complete DNA sequence of the long unique region in the genome of herpes simplex virus type 1. *J. Gen. Virol.* **69**:1531-1574.
- Newcomb, W. W., and J. C. Brown. 1988. Use of Ar⁺ plasma etching to localize structural proteins in viruses: studies with adenovirus 2. *Anal. Biochem.* **169**:279-286.
- Newcomb, W. W., J. C. Brown, F. P. Booy, and A. C. Steven. 1989. Nucleocapsid mass and capsomer protein stoichiometry in equine herpesvirus 1: scanning transmission electron microscopic study. *J. Virol.* **63**:3777-3783.
- Newcomb, W. W., T. A. Johnston, and J. C. Brown. 1987. Ar⁺ plasma etching of palmitic acid multilayers: differential erosion rates of exposed and protected layers. *Langmuir* **3**:1000-1004.
- Perdue, J., J. Cohen, M. Kemp, C. Randall, and D. O'Callaghan. 1975. Characterization of three species of nucleocapsids of equine herpes virus type 1. *Virology* **64**:187-205.
- Perdue, M. L., J. C. Cohen, C. C. Randall, and D. J. O'Callaghan. 1976. Biochemical studies on the maturation of herpesvirus nucleocapsid species. *Virology* **74**:194-208.
- Preston, V. G., J. A. V. Coates, and F. J. Rixon. 1983. Identification and characterization of a herpes simplex virus gene product required for encapsidation of virus DNA. *J. Virol.* **45**:1056-1064.
- Rixon, F. J., A. M. Cross, C. Addison, and V. G. Preston. 1988. The products of herpes simplex virus type 1 gene UL26 which are involved in DNA packaging are strongly associated with empty but not with full capsids. *J. Gen. Virol.* **69**:2879-2891.
- Roizman, B., and D. Furlong. 1974. The replication of herpesviruses, p. 229-403. In H. Fraenkel-Conrat and R. R. Wagner (ed.), *Comprehensive virology*, vol. 3. Plenum Publishing Corp., New York.
- Schrag, J. D., B. V. Prasad, F. J. Rixon, and W. Chiu. 1989. Three-dimensional structure of the HSV-1 nucleocapsid. *Cell* **56**:651-660.
- Sherman, G., and S. L. Bachenheimer. 1988. Characterization of intranuclear capsids made by ts morphogenic mutants of HSV-1. *Virology* **163**:471-480.

23. **Thomas, D., W. W. Newcomb, J. C. Brown, J. S. Wall, J. F. Hainfeld, B. L. Trus, and A. C. Steven.** 1985. Mass and molecular composition of vesicular stomatitis virus: a scanning transmission electron microscopy analysis. *J. Virol.* **54**:598-607.
24. **Vernon, S., M. Ponce de Leon, G. Cohen, R. Eisenberg, and B. Rubin.** 1981. Morphological components of herpesvirus. III. Localization of herpes simplex virus type 1 nucleocapsid polypeptides by immune electron microscopy. *J. Gen. Virol.* **54**:39-46.
25. **Wildy, P., W. Russell, and R. Horne.** 1960. The morphology of herpes virus. *Virology* **12**:204-222.
26. **Zweig, M., C. Heilman, Jr., and B. Hampar.** 1979. Identification of disulfide-linked protein complexes in the nucleocapsids of herpes simplex virus type 2. *Virology* **94**:442-450.